

High-sensitivity methane monitoring based on quasi-fundamental mode matched continuous-wave cavity ring-down spectroscopy

Zhe Li(李哲), Shuang Yang(杨爽), Zhirong Zhang(张志荣), Hua Xia(夏滑), Tao Pang(庞涛), Bian Wu(吴边), Pengshuai Sun(孙鹏帅), Huadong Wang(王华东), and Runqing Yu(余润磬)

Citation: Chin. Phys. B, 2022, 31 (**9**): 094207. DOI: 10.1088/1674-1056/ac5d33
Journal homepage: http://cpb.iphy.ac.cn; http://iopscience.iop.org/cpb

What follows is a list of articles you may be interested in

Nonreciprocal coupling induced entanglement enhancement in a double-cavity optomechanical system

Yuan-Yuan Liu(刘元元), Zhi-Ming Zhang(张智明), Jun-Hao Liu(刘军浩), Jin-Dong Wang(王金东), and Ya-Fei Yu(於亚飞)
Chin. Phys. B, 2022, 31 (**9**): 094203. DOI: 10.1088/1674-1056/ac6499

Bound states in the continuum on perfect conducting reflection gratings

Jianfeng Huang(黄剑峰), Qianju Song(宋前举), Peng Hu(胡鹏), Hong Xiang(向红), and Dezhuan Han(韩德专)
Chin. Phys. B, 2021, 30 (**8**): 084211. DOI: 10.1088/1674-1056/abeee4

Optical nonreciprocity in a piezo-optomechanical system

Yu-Ming Xiao(肖玉铭), Jun-Hao Liu(刘军浩), Qin Wu(吴琴), Ya-Fei Yu(於亚飞), Zhi-Ming Zhang(张智明)
Chin. Phys. B, 2020, 29 (**7**): 074204. DOI: 10.1088/1674-1056/ab8abf

Double-passage mechanical cooling in a coupled optomechanical system

Qing-Xia Mu(穆青霞), Chao Lang(郎潮), Wen-Zhao Zhang(张闻钊)
Chin. Phys. B, 2019, 28 (**11**): 114206. DOI: 10.1088/1674-1056/ab48f1

Controllable optical response in hybrid opto-electromechanical systems

Jiang Cheng, Cui Yuan-Shun, Liu Hong-Xiang, Li Xiao-Wei, Chen Gui-Bin
Chin. Phys. B, 2015, 24 (**5**): 054206. DOI: 10.1088/1674-1056/24/5/054206

High-sensitivity methane monitoring based on quasi-fundamental mode matched continuous-wave cavity ring-down spectroscopy

Zhe Li(李哲)[1,2], Shuang Yang(杨爽)[1], Zhirong Zhang(张志荣)[1,3,4,†], Hua Xia(夏滑)[1], Tao Pang(庞涛)[1], Bian Wu(吴边)[1], Pengshuai Sun(孙鹏帅)[1], Huadong Wang(王华东)[1], and Runqing Yu(余润磬)[1,2]

[1] *Anhui Provincial Key Laboratory of Photonic Devices and Materials, Anhui Institute of Optics and Fine Mechanics, HFIPS, Chinese Academy of Sciences, Hefei* 230031, *China*

[2] *University of Science and Technology of China, Hefei* 230026, *China*

[3] *Key Laboratory of Environmental Optics and Technology, Anhui Institute of Optics and Fine Mechanics, HFIPS, Chinese Academy of Sciences, Hefei* 230031, *China*

[4] *Advanced Laser Technology Laboratory of Anhui Province, Hefei* 230037, *China*

(Received 3 December 2021; revised manuscript received 7 March 2022; accepted manuscript online 14 March 2022)

Continuous-wave cavity ring-down spectroscopy (CW-CRDS) is an important technical means to monitor greenhouse gases in atmospheric environment. In this paper, a CW-CRDS system is built to meet the needs of atmospheric methane monitoring. The problem of mode matching is explained from the perspective of transverse mode and longitudinal mode, and the influence of laser injection efficiency on measurement precision is further analyzed. The results of cavity ring-down time measurement show that the measurement precision is higher when the laser is coupled with the fundamental mode. In the experiment, DFB laser is used to calibrate the system with standard methane concentration, and the measurement residual is less than $\pm 4 \times 10^{-4}$ μs^{-1}. The methane concentration in the air is monitored in real time for two days. The results show the consistency of the concentration changes over the two days, which further demonstrates the reliability of the system for the measurement of trace methane. By analyzing the influence of mode matching, it not only assists the adjustment of the optical path, but also further improves the sensitivity of the system measurement.

Keywords: continuous-wave cavity ring-down spectroscopy (CW-CRDS), cavity modes, coupling efficiency, mode matching, greenhouse gas

PACS: 42.62.Fi, 42.55.Px, 42.79.–e, 42.25.Hz **DOI:** 10.1088/1674-1056/ac5d33

1. Introduction

The Conference of the Parties to the United Nations Framework Convention on Climate Change (UNFCCC)[1] held in Paris proposed that climate change is caused by changes in the level of greenhouse gases in the atmosphere. Accurate access to atmospheric greenhouse gases data will be the primary problem to help the world solve the climate crisis. However, the concentrations of many greenhouse gases[2–5] in the atmosphere are only ppm or even ppb, such as methane ($\sim$ 2 ppm), nitrous oxide ($\sim$ 330 ppb), and carbon monoxide ($\sim$ 30 ppb). When measuring these ultra-trace gases, more sensitive monitoring techniques are required,[6–9] such as cavity-enhanced absorption spectroscopy (CEAS),[10] and quartz-enhanced photoacoustic spectroscopy (QEPAS)[11] technology.

In the past ten years, cavity ring-down absorption spectroscopy[12–14] (CRDS) and off-axis integrated cavity absorption spectroscopy[15–17] (OA-ICOS) were developed for high-precision and high-sensitivity gas measurement. Among them, the OA-ICOS technology requires the use of a larger diameter mirror to improve the power stability of the cavity, allowing multiple beams to be distributed in a larger mirror area, thereby reducing mutual interference between them, and eliminating the mode's influence on the measurement results. The OA-ICOS technology obtains the absorption spectrum of the measured substance through frequency scanning, and consequently the stability of the light source intensity is very important for the measurement. The CRDS technology uses a coaxial optical path, which can make the laser resonate with the fundamental mode by scanning the laser frequency or scanning the cavity length. When the light field in the cavity becomes stable, the acousto-optic modulator (AOM) and other optical switch elements quickly cut off the light source, and the gas concentration can be obtained by measuring the attenuation rate of the light field in the cavity. Compared with the OA-ICOS technology, the advantages of CRDS technology are that the measurement is not affected by light intensity fluctuations, and it has a smaller volume under the same optical path length.

According to the physical mechanism of CRDS, the coupling parameter C_p is the key factor affecting the final detection signal. In CRDS technology, when the laser is coupled into the optical cavity, the coupling efficiency between laser and cavity needs to be considered. The value of C_p depends on the state of mode matching. And the mode matching is determined by the laser, the cavity and the matching degree between them. By analyzing the influence of the mode matching,

†Corresponding author. E-mail: zhangzr@aiofm.ac.cn

© 2022 Chinese Physical Society and IOP Publishing Ltd

the optical path adjustment can be assisted, and the sensitivity of the system measurement can be improved. Generally, mode matching[18,19] includes transverse mode matching and longitudinal mode matching. Some groups have conducted relevant research on mode matching, for example, MIT professor Shaoul Ezekiel[20] used helium-neon light to observe the pattern of the transmitted light spot to help the incident light align with the optical cavity by tuning the cavity length. Xue Ying *et al.*[21] also proposed a cavity adjustment method based on monitoring of transmission spot shape.

The transverse mode matching and longitudinal mode frequency matching in the continuous-wave cavity ring-down spectroscopy measurement system are described. Combined with the experimental results, the matching effect of the incident light and the cavity mode is analyzed. Meanwhile, with the help of an infrared camera, the transmission spots under different conditions are recorded, and the change of resonance signals are observed at the same time. By comparing the cavity ring-down time of different matching modes, the best matching state is confirmed. Then, the cavity ring-down measurement system is calibrated and the measurement error analysis is also performed by measuring different concentrations of methane gas. Finally, the concentration of methane in the atmosphere is monitored for two days. The results indicate that the system is feasible for the measurement of trace methane in the atmosphere.

2. Theory and experiment

2.1. Cavity ring-down spectroscopy

The cavity mirrors generally used for CRDS are high reflectivity mirrors, $R = 99.99\%$. When the laser passes through the first mirror, only 10^{-4} of the power enters the cavity, and most of the rest is reflected. The transmitted light intensity detected by the detector during cavity ring-down is determined by the following equation:[22]

$$I_{\mathrm{t}}(t) = I_{\mathrm{in}} T \exp\left[-\frac{tc}{L}(1-R+\alpha L)\right], \tag{1}$$

where I_{in} is the light intensity injected into the cavity, c is the velocity of light, t is the time, L is the cavity length, α is the absorption of the medium, R is the reflectance and T is the transmittance (relative to intensity).

The 1/e decay time of this exponentially decaying light intensity is called the ring-down time τ, which is defined as

$$\tau = \frac{L}{c(1-R+\alpha L)}, \tag{2}$$

where $\alpha = \sigma N$ is the absorption of the gas including the absorption cross-section σ and the concentration N. Thus, information of the absorbing medium such as the concentration can be obtained through the measurement of the ring-down time.

The detection signal I_{t} is mainly determined by I_{in} and the gas absorption from Eq. (1). The precision of the system can be effectively improved by analyzing the influencing factors of I_{in}. For a stable continuous laser source I_{laser}, light power is continuously injected into the cavity. In order to simply describe the continuous change of intra-cavity light intensity I_{in}, parameters such as wavelength and electric field phase can be ignored. The equation of the light intensity in the cavity is[23]

$$\frac{\mathrm{d}I_{\mathrm{in}}}{\mathrm{d}t} = \frac{c}{2L}[I_{\mathrm{laser}} C_{\mathrm{p}} T - 2I_{\mathrm{in}}(1-R+\alpha L)]. \tag{3}$$

For a cavity with $\alpha = 0$, $t = 0$, $I_{\mathrm{in}} = 0$, the solution of Eq. (3) is

$$I_{\mathrm{in}} = \frac{I_{\mathrm{laser}} C_{\mathrm{p}} T}{2(1-R)}[1-\exp(-t/\tau)]. \tag{4}$$

The light power in the cavity reaches saturation state with time, and the saturation time is equal to the ring-down time, which is

$$\tau_0 = \frac{L}{c(1-R)}. \tag{5}$$

With the saturated state, the intra-cavity light power is expressed as

$$I_{\mathrm{in}} = \frac{I_{\mathrm{laser}} C_{\mathrm{p}} T}{2(1-R)}. \tag{6}$$

Assuming $R + T \approx 1$, Eq. (6) is rewritten as

$$I_{\mathrm{in}} = \frac{I_{\mathrm{laser}} C_{\mathrm{p}}}{2}. \tag{7}$$

For the transmitted light intensity, only a transmission factor is added, which is expressed as

$$I_{\mathrm{t}} = \frac{I_{\mathrm{laser}} C_{\mathrm{p}} T}{2}. \tag{8}$$

When the light source is stable and continuous, the intensity of transmitted light is determined by the cavity coupling parameter C_{p} and the transmittance T. Generally, the reflectivity of the cavity mirror used in CRDS is 99.99%, and the transmittance is only 10^{-4}. C_{p} depends on the spatial mode quality of the light source and the degree of mode matching between the cavity and the laser, and the value is between 0 and 1. The DFB laser is generally used as light source in CW-CRDS, and the output beam is the fundamental mode with good quality. Therefore, C_{p} is greatly affected by the coupling angle, which can also be said to be affected by the mode matching state. Good mode matching can effectively improve the value of C_{p}, and improve the signal-to-noise ratio of detection and the measurement precision of the system. The mode matching in CRDS is analyzed from two perspectives below.

2.1.1. Transverse mode matching

It is known that the DFB laser itself is a resonant cavity and outputs a Gaussian beam. Transverse mode matching mainly refers to the matching between the Gaussian beam waist of the laser and the beam waist of cavity mode. In certain instances, having a mis-aligned cavity will activate many types of transverse cavity modes, which results in a multi exponential decay. The transverse modes that can be excited in the cavity include fundamental modes (TEM_{00}) and many higher-order modes (TEM_{mn}, $m,n = 1,2,3,\ldots$). Better mode matching (with TEM_{00}) of the laser light into the cavity and better detection system could improve the sensitivity.

Usually, a coupling lens (like f in Fig. 1) is used in the optical path to achieve transverse mode matching. After the Gaussian beam passes through the matching lens, its optical properties change. The beam waist size and position are equal to those of the cavity mode. And the wavefront is the same as the curvature of the cavity mirror. As shown in the schematic diagram of Fig. 1, a lens with a suitable focal length is selected to make the two beam waists form an object-image relationship, so as to achieve transverse mode matching.

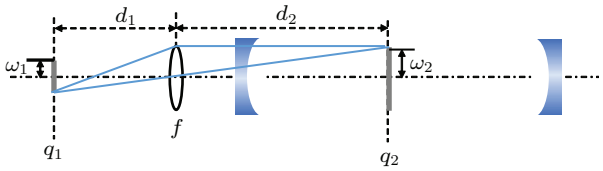


Fig. 1. Schematic diagram of transverse mode matching.

As shown, q_1 represents the beam waist of the laser, and ω_1 is the radius of beam waist. q_2 is the waist of the cavity mode and ω_2 is the radius of waist. The distances between the lens f and the waist beams ω_1 and ω_2 are d_1 and d_2, respectively. The object-image relationship satisfied by ω_1 and ω_2 is

$$\frac{\omega_1}{\omega_2} = \frac{d_1}{d_2} = \frac{d_1 - f}{f}, \tag{9}$$

where f is the focal length of the matching lens. According to the various parameters of the system, a matching lens with a focal length of 4.6 mm is selected. This method of transverse mode matching is applicable to both linear resonant cavities and more complex resonant cavity structures.

2.1.2. Longitudinal mode frequency matching

The longitudinal mode frequency matching is mainly the matching between the incident light frequency and the cavity mode frequency, especially TEM_{00q}. Longitudinal mode matching must meet two points. One is that the frequency of the laser is an integer multiple of the free spectral region (FSR) of the cavity, and the other is that the linewidth of the laser is equal to or equivalent to the linewidth of the cavity's longitudinal mode. The generally used CW DFB laser has a very narrow line width, which is much smaller than FSR. Therefore, wavelength scanning[24] or cavity length scanning is often used to achieve period matching and improve matching efficiency. The fundamental mode TEM_{00q} and the higher-order mode TEM_{mnq} are intrinsic modes of the cavity, which are determined by the characteristics of the cavity, cavity length L and radius of curvature R_c. In the cavity, a standing wave is formed along the axis of the cavity, and the node of the standing wave is determined by q. The field distribution of the standing wave is called the longitudinal mode, and q (positive integer) is the ordinal number of the longitudinal mode. The difference between the frequencies of two adjacent longitudinal modes is called the frequency interval of the longitudinal mode ($\Delta\nu_{00q}$) or free spectral region (FSR),

$$\Delta\nu_{00q} = \mathrm{FSR} = \frac{c}{2L}.$$

The frequency in the cavity that meets the resonant condition is called the resonant frequency, which is expressed as

$$\nu_{mnq} = \frac{c}{2L}(q+1) + \frac{(m+n+1)}{\pi}\arccos\left(1 - \frac{L}{R_c}\right), \tag{10}$$

where m and n are both positive integers, standing for the order of the transverse mode. The factor $g = \sqrt{1 - L/\rho}$ characterizes the stability of the cavity. The distribution of modes in the cavity is simulated according to the experimental parameters, and the results are shown in Fig. 2.

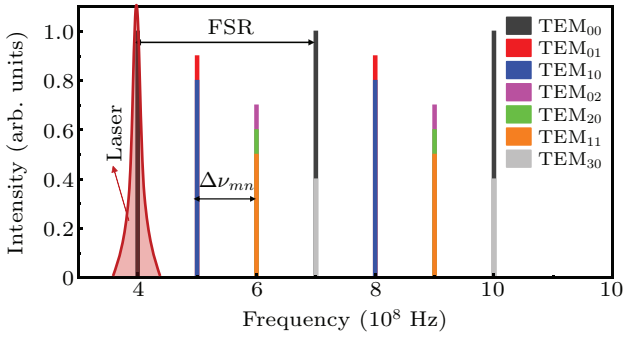


Fig. 2. Simulation of resonant frequency of the cavity.

The simulation result gives a longitudinal mode spacing FSR = 300 MHz, and a transverse mode spacing of $\Delta\nu_{mn}$ =100 MHz. It can be seen form Eq. (10) that there is an equivalent relationship between m and n. The simulation results show that the TEM_{01q} and TEM_{10q} modes are degenerate, so are the TEM_{02q}, TEM_{20q}, and TEM_{11q} modes. The degenerate modes satisfy the relationship of $m+n = 3\times k$ ($k = 1$, 2, 3, ...). In addition to the results shown by the simulation, there are more high-order modes that are degenerate. Excessively high-order modes can be eliminated by reducing the size of the cavity mirror or adding a small hole in the cavity. In the experiment, tuning the frequency of the laser to match the cavity mode, and the matching with fundamental mode TEM_{00q}

is the best. It is always the quasi-fundamental mode matching state in fact, with the TEM_{01q} and TEM_{10q} modes also participating in the mode matching.

2.2. Cavity ring-down system

The schematic diagram of continuous wave CRDS measurement system based on linear optical cavity is shown in Fig. 3. The distributed feedback laser (DFB) is used as the light source, and the driving current is controlled by LabVIEW software. The modulated laser passes through the optical fiber isolator and acousto-optic modulator (AOM), and then couples into the optical cavity through the matching lens. The instantaneous matching between the incident light frequency and the cavity mode frequency is realized by scanning the laser frequency. When the optical power in the cavity reaches the set threshold, the control board immediately sends a command to turn off the laser to the AOM. The optical power in the cavity decreases gradually with time. So, the information of the absorbing medium in the cavity is characterized by measuring the attenuation schedule of optical power. It is worth noting that the light intensity attenuation time is only microseconds, so it has high requirements for the speed of the acquisition card and the sensitivity of the photodetector.

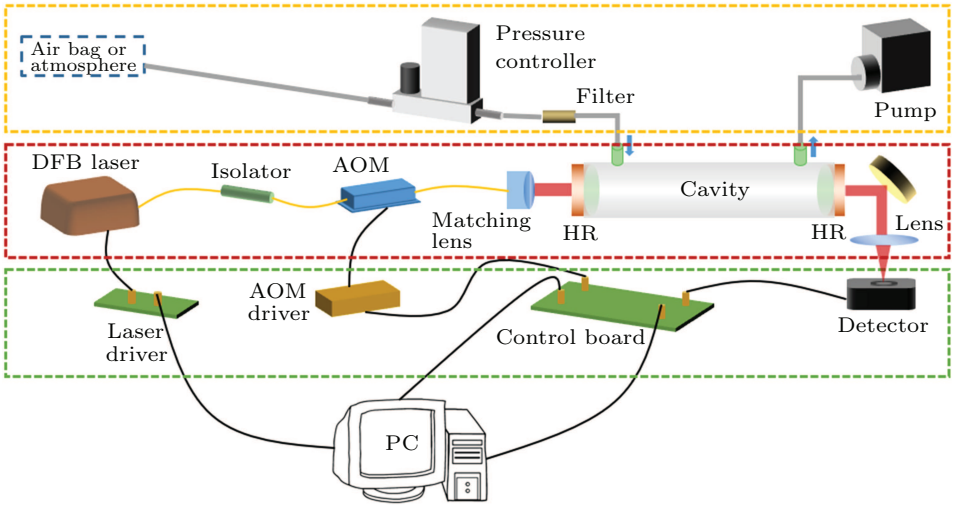


Fig. 3. Schematic diagram of cavity ring-down system.

3. Results and discussion

3.1. Mode matching experimental measurement

In the experiment, a matching lens is used to achieve transverse mode matching. The lens is installed on a five-dimensional adjustment frame to facilitate fine adjustment of the incident angle into the optical cavity. As shown in Fig. 4, there is a spatial distance between the lens and the optical cavity. According to the beam waist matching relationship and the parameters of the experimental system, the matching lens with focal length of 4.6 mm is selected, and the spatial distance is 7.7 cm. It is necessary to adjust the spatial beam to match the optical cavity to complete the high-efficiency coupling.

In this part, the transverse matching and longitudinal mode matching are combined to analyze the mode matching and mode mismatch between the incident laser and the optical cavity. In order to observe the actual change state of the transverse mode more intuitively, the infrared camera (Xenics, Bobcat-640) is placed at the transmission mirror of the cavity. The camera is used to observe the shape changes of the transmitted light spot in real time, and at the same time refer to the resonance signal recorded by the oscilloscope to judge the alignment. During the experiment, the scanning frequency of the laser is 140 Hz, and the infrared camera is able to capture continuous changes in the transverse mode light spot. Figure 5 shows the modes are observed in the state of quasi-fundamental mode matching. As shown in the figure, the transverse modes represented by the subgraph are (a) TEM_{00}, (b) TEM_{01}, (c) TEM_{10}, (d) TEM_{11}, (e) transition state between TEM_{01} and TEM_{11}, (f) TEM_{02}.

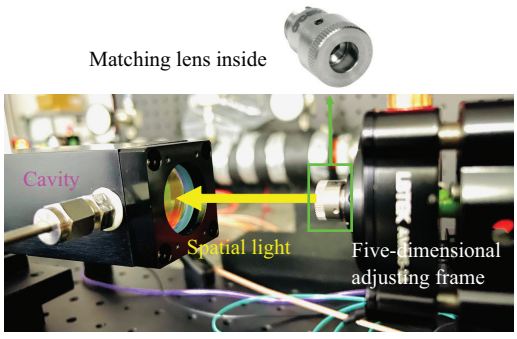


Fig. 4. System structure of matching lens.

According to the observation of the light spot change in the experiment, it is found that when the incident light enters the optical cavity normally, the most ideal resonance state is obtained. The fundamental mode TEM_{00q} is excited, and

the transverse mode light spot flashes continuously as shown in Fig. 5(a). Of course, due to the instability of the optical cavity structure or the drift of the laser frequency, occasionally a low-order high-order transverse mode pattern will appear, as shown in Fig. 5(b). In general, the probability of the light spot in Fig. 5(a) is the largest. The matching state at this time is quasi-fundamental mode matching. The resonant signal in the cavity is observed as shown in Fig. 6(a). There are three modes are excited in a FSR spacing, but only one excited mode has the largest amplitude. The matching state of this quasi-fundamental mode is the most ideal matching state of the system.

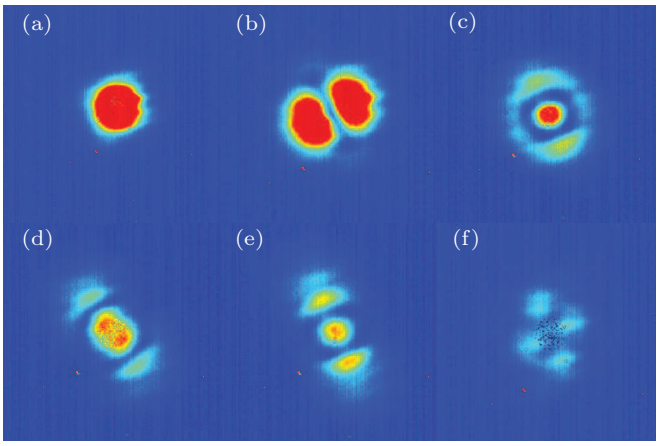


Fig. 5. Transverse mode spot taken by infrared camera: (a) fundamental mode, TEM_{00q} (b)–(f) high-order transverse mode, TEM_{mnq}.

When the injection angle of the beam is changed slightly, the coaxial incidence is no longer sufficient. The transmitted light spots appear in various shapes, and some low-order spot modes are shown in Figs. 5(a)–5(f). The appearance of the higher-order mode spot indicates that they are also excited. The infrared camera photographed a lower-order mode with a greater probability of appearing. Also in the resonant signal (Fig. 6(b)), the high-order mode indicated by the arrow has a large amplitude. Compared with the signal of quasi-fundamental mode matching, the overall amplitude of high-order mode matching is reduced. It can be seen from Fig. 6(b) that the three modes exceeding the preset threshold can trigger the AOM to cut off the laser and generate ring-down events. These signals are also collected and processed as effective signals. This is the so-called "misjudgment" in the threshold comparison.

For the occurrence of this kind of mismatch, it can also be solved by increasing the judgment threshold. For example, in Fig. 6, the red line threshold should be increased to about 1.0. But, it is also found that once the higher-order mode is excited, its amplitude is often very high or even higher than the excited fundamental mode. Therefore, this situation cannot be avoided by simply increasing the threshold completely.

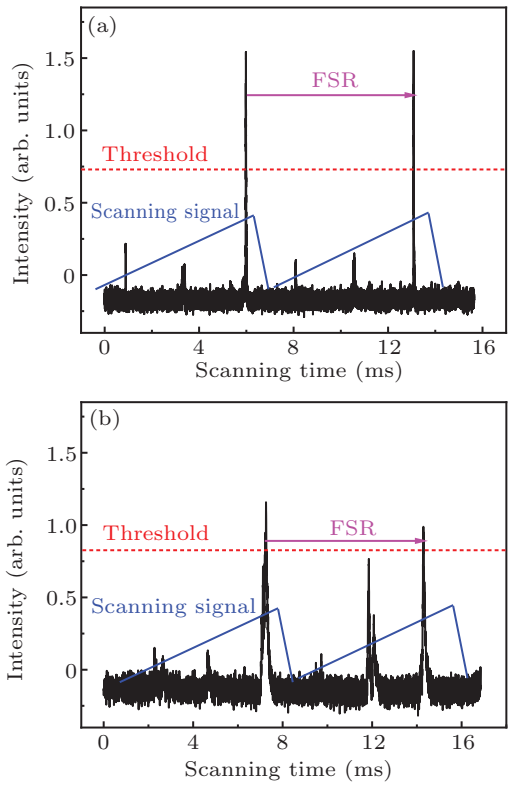


Fig. 6. The resonant signal of mode matching: (a) quasi-fundamental mode matching; (b) high-order mode matching, the scanning period is 2FSR.

In order to explain the influence of the two states of mode matching (fundamental mode and higher-order mode) on the measurement results when they are excited. The values of cavity ring-down time (τ) are continuously collected with two matching states, and the results of 1000 sets of data is shown in Fig. 7. It can be seen that in the matching state of the quasi-fundamental mode, the measured cavity ring-down time is $17.121. \pm 0.051$ μs. And in the high-order mode matching, the cavity ring-down time ($15.332. \pm 1.121$ μs) is reduced because the increased cross-section of the mode causes more loss. Therefore, the quasi-fundamental mode matching has a higher measurement accuracy and precision, compared with the theoretical value (18.519 μs).

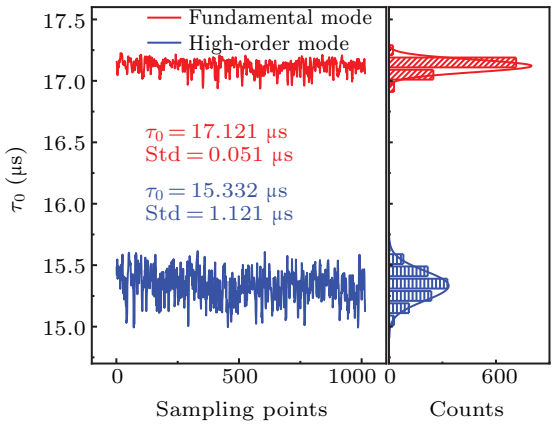


Fig. 7. Measurement of cavity ring-down time (red: quasi-fundamental mode matching, blue: high-order mode matching).

In addition, TEM_{00q} has the highest coupling efficiency and the highest transmitted light intensity in the quasi-fundamental mode matching. The results show that the higher precision of the quasi-fundamental mode matching, the smaller fluctuation of the measurement results. This is also the most concerned issue of the research. With quasi-fundamental mode matching, the standard deviation is only 0.051 μs and the precision of detection is 0.037 ppm (without average). The measurement precision can be improved to 3.3 ppb with average of 32 times. In contrast, TEM_{01q}, TEM_{10q} and even higher-order modes are excited to a strong level and trigger the threshold. Since the modes of different orders have different losses, different ring-down times are obtained with the measurement fluctuation of 0.121 μs. These also fully prove that the measurement precision of quasi-fundamental mode matching is better, which can greatly reduce the measurement error and improve the measurement precision.

3.2. Measurement results of methane

In the experiment, a 1653 nm continuous DFB laser is used as the detection light source. The frequency modulation method is adopted to improve the matching efficiency. This method is to scan the CH_4 absorption line with a small amplitude. 1653.72 nm is selected as the central spectral line of CH_4 measurement, where the absorption interference of other gases is the smallest and can be ignored during measurement.

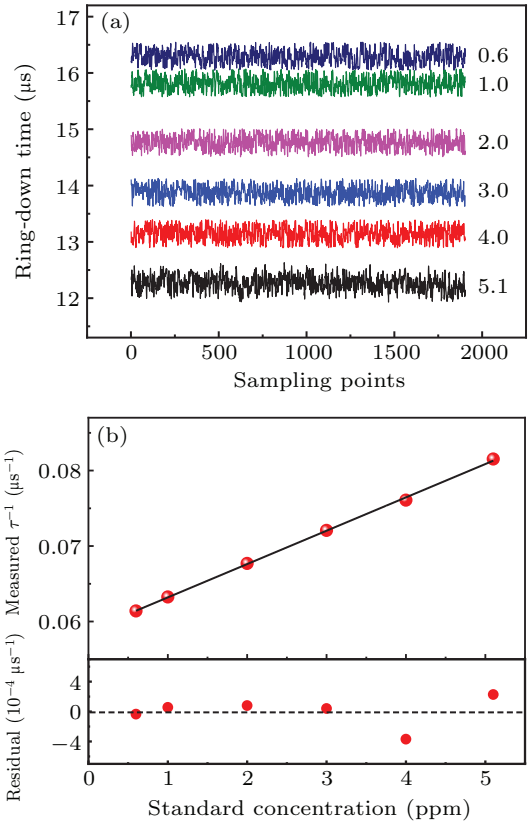


Fig. 8. (a) The ring-down time measurement of different concentrations of CH_4. (b) Linearity of the system.

The different CH_4 standard concentration gases (5.1 ppm, 4.0 ppm, 3.0 ppm, 2.0 ppm, 1.0 ppm, and 0.6 ppm, Nanjing Special Gas) are measured to calibrate the system. The measurement results of the ring down time are shown in Fig. 8(a). The above measurements are carried out in a stable environment. In Fig. 8(a), 1900 sets of data are measured for each standard concentration of CH_4. The relationship between the measured value and the standard value is shown in Fig. 8(b). The fitting is given by $y = 0.0588 + 0.0044x$ with 0.99 fitting coefficient (R-square). The relative error can be obtained from the standard concentration and fitting concentration. And the measurement residual is less than $\pm 4 \times 10^{-4}$ μs^{-1}, which basically meets the measurement requirements.

The calibrated system will be used to monitor the CH_4 in the air. The CH_4 gas in the laboratory air is measured for two consecutive days. The measured concentration fluctuates regularly and periodically over the two days, which are shown in Fig. 9. During measurement, the air pump system is used to pump air into the cavity continuously and slowly. The detecting frequency is stabilized at the position of the methane absorption peak.

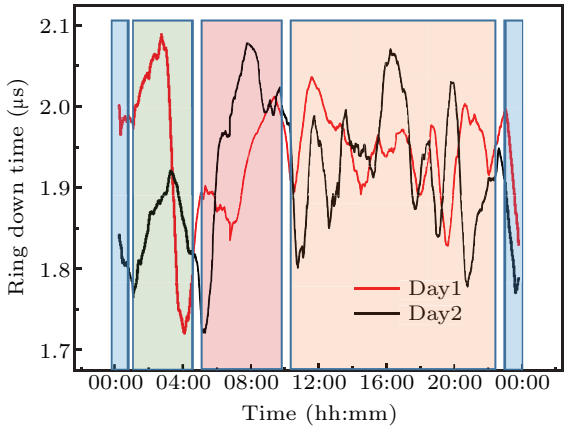


Fig. 9. Monitoring of methane in the air.

During the period of 1:00∼5:00, the concentration of CH_4 increases but later decreases. CH_4 concentration shows an obvious upward trend at the period of 5:00∼10:00. Between 10:00 and 22:00, the concentration of CH_4 has the sever fluctuation. During the period of 22:00∼1:00 (+24), CH_4 concentration shows a downward trend. It is inferred that the concentration change trend is related to human activities and other factors. Comparing the two-day measurement results, it shows the consistency of the change trend of CH_4 concentration, and verifies the feasibility of the experimental system.

4. Conclusion

In this paper, the coupling between the different cavity modes and laser is analyzed, and the existence of different excitation modes is verified in experiments. With the help of infrared camera, the most ideal resonant state quasi-fundamental

mode matching is obtained. In the two matching states, the ring-down times and standard deviations are 17.121. ± 0.051 μs and 15.332. ± 1.121 μs, respectively. Therefore, the measurement precision of quasi-fundamental mode matching is better, which can greatly reduce the measurement error and improve the precision of the system. Therefore, based on the above analysis, it is summarized as follows: In the CRDS measurement technology, a lens with an appropriate focal length is selected according to the optical cavity parameters to achieve the mode matching between the laser beam and the cavity mode. Under the premise of high coaxiality, the frequency scanning method increases the resonant efficiency of the laser and the fundamental mode in the cavity. The precision adjustment of the laser and the cavity makes the measurement result more precise and more sensitive. During the coaxial adjustment of the optical path, the change in the state of the transverse mode can be observed by the infrared camera, which improves the efficiency of optical path alignment. So, mode matching is a basic but vital part of the cavity ring-down system, which lays the foundation for the subsequent development of cavity ring-down technology for high-sensitivity detection of trace gases. In this paper, the precision is discussed in mode matching, and the measurement accuracy and system robustness are not studied. These two are the key to the system in practical application. How to evaluate and improve the stability and robustness of the system is the next step.

Acknowledgements

This research is financial supported by the Natural National Science Foundation of China (Grant Nos. 11874364, 41877311, and 42005107), the National Key Research and Development Program of China (Grant No. 2017YFC0805004), and the CAS & Bengbu Technology Transfer Project (Grant No. ZKBB202102).

References

[1] Wang J D, Yu J and Mo Z Q 2019 *Spectroscopy Spectral Anal.* **39** 2046
[2] Mchale L E, Martinez B, Miller T W, *et al.* 2019 *Opt. Express* **27** 20084
[3] Hodges J T, Layer H P and Miller W W 2004 *Rev. Scient. Instrum.* **75** 849
[4] Wang J D, Yu J, Mo Z Q, *et al.* 2019 *Acta Phys. Sin.* **68** 244201 (in Chinese)
[5] Yang Z H, Yang Y C and Deng L Z 2018 *Chin. Phys. B* **27** 164
[6] Wang Z, Wang Q and Zhang W 2019 *Opt. Lett.* **44** 1924
[7] Chen J, Fullam D P and Yu S S 2019 *Spectrochimica Acta Part A* **218** 178
[8] Lyulin O M, Kassi S and Campargue A 2021 *J. Quant. Spectroscopy Radiative Transfer* **271** 107733
[9] Wu H, Dong L and Zheng H 2017 *Nat. Commun.* **8** 15331
[10] Lei D, Li C and Sanchez N P 2016 *Appl. Phys. Lett.* **108** 11106
[11] Wei T T, Zifarelli A and Russo S D 2021 *Appl. Phys. Rev.* **8** 41409
[12] Wang J, Yu J and Mo Z 2019 *Appl. Opt.* **58** 2773
[13] Stowasser C, Farinas A D and Ware J 2014 *Appl. Phys. B* **116** 255
[14] Chen T L, Ober D C and Miri R 2021 *Analytical Chem.* **93** 6375
[15] Wang J, Tian X and Dong Y 2019 *Opt. Express* **27** 30517
[16] Zheng K, Zheng C and Yao D 2019 *Analyst* **144** 2003
[17] Clouser B W, Sarkozy L and Moyer E J 2018 *Appl. Opt.* **57** 6252
[18] Huang H F and Lehmann K K 2007 *Opt. Express* **15** 8745
[19] Hodges J T, Layer H P and Miller W W 2004 *Rev. Scient. Instrum.* **75** 849
[20] Meyer R E, Sanders G A and Ezekiel S 1983 *J. Opt. Soc. Amer.* **73** 939
[21] Xue Y, Du X H and He X 2020 *Chin. J. Lasers* **47** 415
[22] Scherer J J, Paul J B and O'Keefe A 1997 *Chem. Rev.* **97** 25
[23] Paul J B, Lapson L and Anderson J G 2001 *Appl. Opt.* **40** 4904
[24] Wang Z, Du Y J and Ding Y J 2019 *Acta Phys. Sin.* **68** 204204 (in Chinese)